ONIOM Study of Ring Opening and Metal Insertion Reactions with Derivatives of C_{60}: Role of Aromaticity in the Opening Process

Stephan Irle,[†] Yves Rubin,[‡] and Keiji Morokuma*[,†]

Cherry L. Emerson Center for Scientific Computation and Department of Chemistry, Emory University, Atlanta, Georgia 30322, and Department of Chemistry and Biochemistry, University of California, Los Angeles, Los Angeles, California 90095-1569

Received: October 23, 2001

We have used the integrated, high accuracy ONIOM(G2MS) molecular orbital method to study the problem of ring-opening and metal-insertions into C_{60}. The concerted ring-opening pathway proposed by Rubin et al. has been examined for hexahydro and hexamethyl derivatives of C_{60}. The related open bistriazoline and bislactam C_{60} derivatives (*Angew. Chem. Int. Ed. Engl.* **1999**, *38*, 2360−2363) have also been studied. In the two possible [2+2+2] ring-fragmentation pathways breaking three sets of either five or six-membered rings, the 5-open hexahydro or hexamethylated species are much more favored than the 6-open analogues, the process being slightly endothermic in respect to the closed species. The orifice generated in these two species are likely to be too small even for the smallest metal cation Li^+, with insertion barriers ranging from 45 to 60 kcal/mol. On the other hand, the Li^+ insertion barriers for the bistriazoline and bislactam derivatives are less than 20 kcal/mol, indicating that this small metal cation should be able to insert into the cavity of these systems with stabilization energies near −10 kcal/mol. These results suggest that a larger orifice is required for one of the desirable transition or f-row metals to be taken inside.

I. Introduction

One of the important goals of current fullerene chemistry is to introduce a metal atom within the empty cavity of C_{60}. The high electron affinity of C_{60} has led to the discovery of a surprising array of physical properties for its salts (e.g., superconductivity in its tri-alkali metal salts, and ferromagnetism in charge-transfer salts with $(Me_2N)_2C{=}C(NMe_2)$).[1,2] The high symmetry of C_{60}, which can impart unique physical properties on its compounds compared to those of the less symmetrical, larger fullerenes (C_{70}, C_{76}, C_{84}, etc.), makes it an attractive goal to incorporate transition or f-row metal atoms within its empty cavity of about 3.5 Å in diameter.[3] With their wide variety of oxidation and spin states, it can be expected that the transition metal complexes within C_{60} will expand the range of useful physical properties for the pristine and functionalized complexes. Several charge-transfer complexes of fullerenes with metal atoms inside have been obtained by the classic arc evaporation method (e.g., La@C_{76}, La@C_{78}, Ln@C_{82} (Ln = La, Y, Sc, Gd, Tm), Sc_2@C_{84}, Sc_3@C_{82}). However, they can be prepared only in very limited quantities, either by evaporation of graphite rods filled with metal oxides,[4] or by beam experiments to generate polymerized films with e.g., Li@C_{60}.[5] More recently, a process giving an exceptionally high yield (up to 10%) of a trilanthanide nitride cluster (Sc_3N@C_{80}) was reported.[5g]

On the other hand, these methods have so far not provided C_{60} endohedrals in pure form,[6] and chemical synthesis appears to be the best alternative to obtain these promising compounds in larger quantities. An ab initio study of direct collisions between lithium atoms and C_{60} as a brute force approach showed that at least 644 kcal/mol are required for the metal atom to squeeze into the cavity through a six-membered ring,[7] which would easily destroy the fullerene's structure.

To overcome these obstacles, Rubin and co-workers have been investigating synthetic approaches to endohedral metallofullerenes that would yield larger quantities of well-defined compounds compared to the methods described above.[3] The key concept is to use chemical transformations that are able to sever several bonds within the framework of C_{60} in order to give a sizable opening. A strategy effecting a retro [2+2+2] cycloaddition reaction of a hexasubstituted fullerene, such as the theoretical structure **H6** (see Figure 1), was proposed for the spontaneous ring opening of 3 bonds, leading to the open forms **H6**−**5o** or **H6**−**6o** depending on whether five- or six-membered rings have been cleaved (see also Figure 2). In fact, similarly strained, 6-fold substituted planar systems are known to undergo this transformation with relatively low activation barriers to produce open trienes.[8] Although the orifice of **H6**−**5o** or **H6**−**6o** is not large enough to let any metal atom or ion pass through, Rubin et al. calculated that vibrational frequencies involving C═C stretches in the opening C_6-moiety were just about 300 cm^{-1},[3] and suggested that the metal could "slip in" under proper thermal activation or pressure. An alternate way to increase the size of the orifice is to use bulkier groups such as methyl substituents (**M6**), wherein steric repulsion between the substituents pushes the nonbonded parts in **M6**−**5o** or **M6**−**6o** even further apart. The original MM3 and semiempirical calculations of this work[3] show a wide range of possible energetics associated with these species (Table 1), and the question remains what structure would be the most promising in this ring opening procedure. From an experimental point of view, the preparation

* To whom correspondence should be addressed. E-mail: morokuma@emory.edu.

[†] Cherry L. Emerson Center for Scientific Computation and Department of Chemistry, Emory University.

[‡] Department of Chemistry and Biochemistry, University of California, Los Angeles.

10.1021/jp0139282 CCC: $22.00
Published on Web 01/08/2002

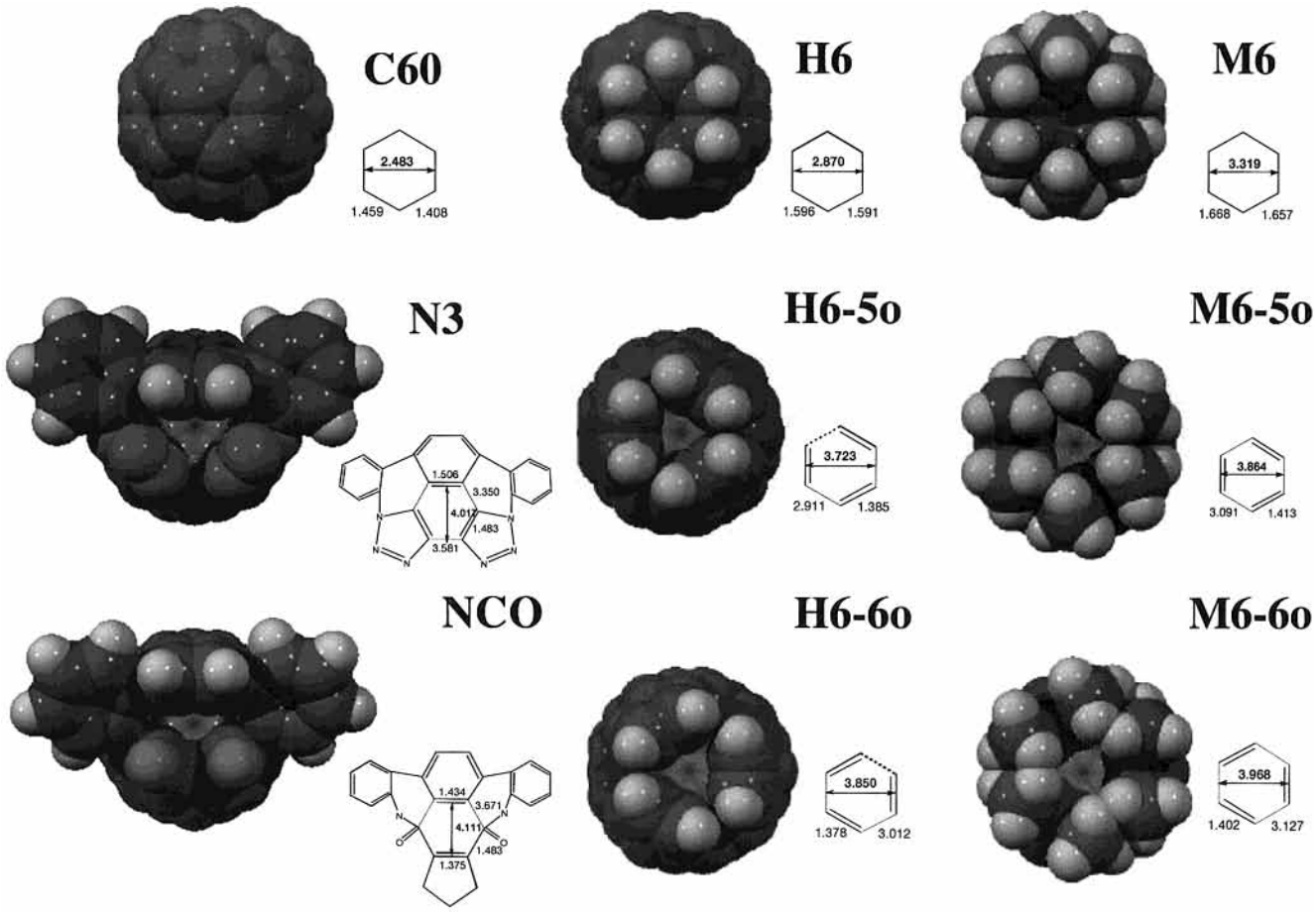

Figure 1. CPK representation and schematic drawings of six-membered ring area of ONIOM2 optimized structures for **H6**, **H6−5o**, **H6−6o**, **M6**, **M6−5o**, **M6−6o**, **N3**, and **NCO**. Distances are in Å.

TABLE 1: Relative Energies (in kcal/mol) between Closed, 5-Opened (-5o) and 6-Opened (-6o) Forms as Well as Those of Li^+ Insertion Transition States for Hexa-hydrogenated C_{60} (H6), Hexa-methylated C_{60} (M6), and C_{60} with Macrocyclic Functional Groups N3 and NCO

system	nimag[a]	AM1[b]	PM3[b]	RHF/3-21G	BP/SVP	ONIOM(G2MS)
H6 + Li$^+$	0	0.0	0.0	0.0	0.0	0.0
H6−5o + Li$^+$	0	9.0	14.1	29.2	19.5	7.1
H6−6o + Li$^+$	0	64.2	56.3	76.8	61.2	45.6
H6−5o···Li$^+$	0					−4.1
H6−56···Li$^+$	0					−3.1
Li$^+$TS H6−5o	1 (a_1:450)			108.6 (79.4[c])		68.2 (61.1)
Li$^+$TS H6−6o	1 (a_1:398)			148.1 (71.3)		96.3 (50.7)
H6−5o@Li$^+$	0					−10.8
H6−6o@Li$^+$	0					−11.7
M6 + Li$^+$	0	0.0	0.0	0.0	0.0	0.0
M6−5o + Li$^+$	0	−36.4	−19.4	6.2	−3.7	1.3
M6−6o + Li$^+$	0	8.3	16.3	50.2	25.7	37.2
M6−6o···Li$^+$	0					−10.5
Li$^+$TS H6−5o	1 (a_1:367)			72.5 (66.3)		51.0 (49.7)
Li$^+$TS H6−6o	1 (a_1:344)			111.7 (61.5)		82.3 (45.1)
M6−5o@Li$^+$	0					−6.3
M6−6o@Li$^+$	0					−7.1
N3-o + Li$^+$	0			0.0	0.0	0.0
Li$^+$TS N3−o	1 (a′:375)			35.6	24.4	19.6
NCO-o + Li$^+$	0			0.0	0.0	0.0
Li$^+$TS NCO−o	1 (a:344)			29.5	22.7	15.7

[a] Nimag is the number of imaginary frequencies. If Nimag is not zero, the actual imaginary frequencies (without *i*, in cm^{-1}) are shown with its irreducible representation. [b] Ref 7b. [c] Values in parentheses are relative energies with respect to the corresponding open structures.

of C_{60} with six individual groups added on a specific single six-membered ring seems extremely difficult to achieve, not only due to the many possibilities that other double bonds may react during the addition process, but also due to severe steric interactions introduced between the adjacent groups.

Recently, Rubin et al. have reported progress in experiments,[9−11] where all three adding groups (diene and 1,3-dipoles partners) are part of a single rigidly preorganized molecule, thus ensuring maximum probability of reaction with one of the six-membered rings of C_{60}. This approach should also diminish the

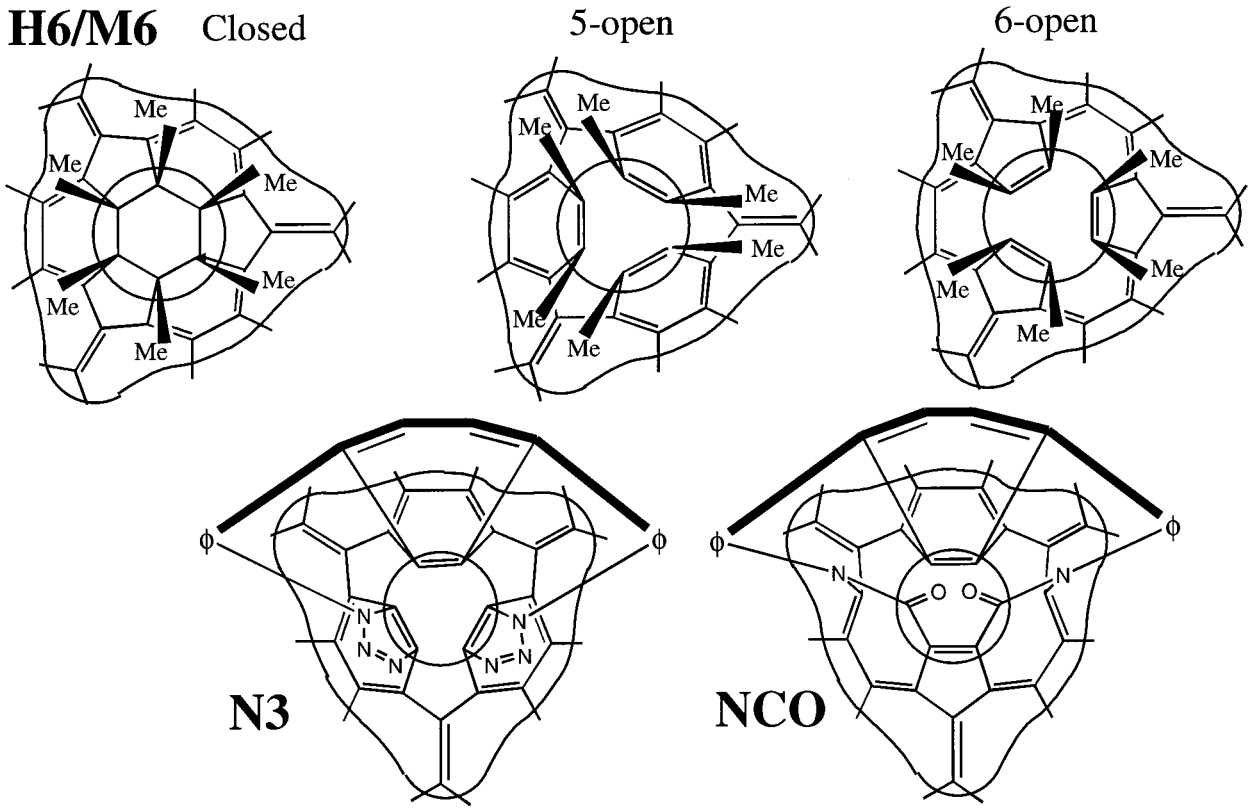

Figure 2. Schematic drawings of the structures and ONIOM models for **H6**, **H6**−**5o**, **H6**−**6o**, **M6**, **M6**−**5o**, **M6**−**6o**, **N3**, and **NCO**. The atoms inside the smaller circle (plus link H atoms) constitute the small model system M and the atoms inside the larger circular curve (plus link H atoms) constitute the intermediate model system I.

steric repulsion between adding groups while a very large orifice could be created upon aromatization (flattening and rigidification) of the breaking units. The role of energetics in these processes is the purpose of this article and is examined with a very high level ONIOM scheme.

There have been numerous electronic structure calculations reported in the literature on fullerenes as well as the metal complexes of endohedral fullerenes.[12] Most of them were performed at semiempirical or density functional levels, with a few exceptions where MP2 was employed.[13] Highly accurate calculations at the G2/G3 or the computationally less demanding G2MP2 level of theory[14,15] are definitely prohibited for these systems due to their size. However, the insertion step of an atom through the orifice is a very local event, and high level calculations are feasible for a model system of e.g., six carbon atoms and the incoming atom.

Integrated methods such as the ONIOM[16] scheme allow to treat a selected area of a larger system at a high level, whereas the rest of the system is treated using a computationally more feasible level of theory. To shed light on the questions mentioned above in relation to atom insertion into C_{60} derivatives, we have performed two and three-layer ONIOM calculations (ONIOM2 and ONIOM3) with G2MS[17] as the highest level of theory, which is well suited to predict highly accurate relative stabilities between five- and six-membered ring open structures. The ONIOM method also is in the position of providing reliable barriers for atom insertion by locating the corresponding transition states. In these calculations, we are treating the chemically modified region of C_{60} at a high level of theory, whereas the electronic structure of the environment is taken into account at a lower level of theory, as described in Section II. Using this approach, we studied closed and open forms of the model compounds hexahydrofullerene (**H6**) and hexamethylfullerene (**M6**), as well as C_{60} with larger addends such as the fullerene bisazide adduct **N3**, and a fullerene bislactam derivative (**NCO**). These systems have been investigated before at the semiempirical AM1 and PM3 levels of theory by Rubin et al.,[9] and our calculations seek to improve the structure and energetics of the processes and assess the accuracy of the semiempirical approaches. To simulate the insertion of metal atoms, we chose Li^+ as the smallest metal ion with a diameter of about 1.46 Å[18] as a probe atom and calculated the transition states for atom insertion. These calculations are similar to recent calculations by Rubin et al., who determined transition states for the insertion of noble gases as well as molecular hydrogen and nitrogen into the bislactam **NCO** by using density functional theory calculations. Additionally, the insertion of helium and molecular hydrogen was investigated experimentally, and the activation barrier for the release of helium was determined. The agreement between density functional theory calculations and experimental barrier of about 24 kcal/mol was excellent, with less than 1 kcal/mol difference.[11] ONIOM allows us to estimate these barriers at an even more accurate level of theory and to clarify if the agreement between the density functional barrier and experiment is fortuitous (the high barrier of H_2 decomplexation, at 40 kcal/mol could not be determined experimentally).

II. Computational Methods

Every structure studied was pre-optimized at the RHF/3-21G level of theory. These systems were then partitioned into two or three ONIOM layers, as shown in Figure 2 and Table 2. The symbol R denotes the real system including all atoms, whereas I stands for the intermediate model system consisting of the next neighbor rings (plus link H atoms that mend the broken bonds) without interrupting any π bonds. The symbol M stands for the small model system, which is naturally the C_6 ring to

TABLE 2: ONIOM Model Structures Employed in 2- and 3-Layer Calculations for Optimizations (ONIOM2) and Energies (ONIOM3)

systems	H6	M6	N3	NCO	ONIOM2	ONIOM3
small model: **M**	C_6H_{12}	C_6H_{12}	C_6H_{12}	$C_6H_8O_2$	MP2/6-31G(d)	G2MS
intermediate model: **I**	$C_{24}H_{12}(H)_6$	$C_{24}H_{12}(CH_3)_6$	$C_{24}H_{12}(N_3H)_2(H)_2$	$C_{24}H_{12}(ONH)_2(H)_2$	RHF/3-21G	MP2/6-31G(d)
real: **R**	$C_{60}H_6$	$C_{60}(CH_3)_6$	$C_{60}(N_3)_2(\phi C_4H_2\phi)^a$	$C_{60}(ON)_2(\phi C_4H_2\phi)$	RHF/3-21G	RHF/3-21G

[a] ϕ = *o*-C_6H_4.

be opened (plus link H atoms that mend the broken bonds) in all the systems but one to be discussed later. A two-layer ONIOM, ONIOM2(MP2/6-31G(d):RHF/3-21G), was employed for geometry optimizations and frequency calculations, using MP2/6-31G(d) for the system M and RHF/3-21G for the R system, whereas three-layer ONIOM, ONIOM3(G2MS:MP2/6-31G(d):RHF/3-21G) was used for single point energy calculations at the ONIOM2 stationary points. The three-layer calculations feature the highly accurate G2MS[17] level of theory for the M system (C_6H_{12}), MP2/6-31G(d) for the I system, and RHF/3-21G for the R system. G2MS itself is an extrapolation scheme which uses RMP2/6-31G(d) as the base and features spin-restricted RCCSD(T)/6-31G(d) as the method to describe high level correlation effects and calculates basis set corrections at the spin-restricted RMP2/6-311+G(2df,2p) level. The G2MS extrapolation method is applicable quite reliably to closed- and open-shell systems. Open-shell systems were involved in this study in calculating binding energies for **H6** and **M6** and treated at the restricted level to avoid spin contamination. For the sake of comparison, we also present a few DFT single point energy results, obtained at the BP/SVP level, i.e., the Becke−Perdew functional[19] using a split valence basis set with polarization functions on carbon,[20] with the resolution-of-identity-approximation (RI-DFT) as implemented in TURBOMOLE[21] for ONIOM2 optimized structures.[22]

The ONIOM3//ONIOM2 approach has been successfully employed before,[23] and we feel comfortable using this 2-fold strategy. In particular, the G2MS:MP2:RHF hierarchy has been demonstrated to give excellent results, as these methods also represent systematic methodological improvement over each other, in contrast to inclusion of DFT as one level of theory.[24] The G2MS method is expected to provide the bond dissociation energies within an error of a few kcal/mol, and the ONIOM3-(G2MS:MP2/6-31G(d):RHF/3-21G) (later also called ONIOM-(G2MS) for brevity) extrapolation is expected to add one kcal/mol or so to this error.[25] Thus, the energetics we obtain in the present paper would be much more reliable than any other single level calculations available or accomplishable soon for the present systems.

We have used GAUSSIAN's implementation of ONIOM, partly employing our own development version, and partly the publicly available versions 98.A1 and 98.A7.[26] Due to the high symmetry of many of the compounds under investigation, symmetry restrictions were applied where possible, namely C_{3v} for hexahydro- and hexamethylfullerenes and C_s for the larger systems **N3** and **NCO**. All systems (except for the binding energy calculation) were treated assuming closed-shell electronic structures. Analytical frequency calculations were then performed for each structure at the ONIOM2 level, to characterize the nature of these stationary points on the PES based on the number of imaginary frequencies (NImag). For the characterization of charge distributions, standard Mulliken population analysis was employed, based on integrated densities of the ONIOM2 level.

III. Results and Discussion

The region for the formation of the orifice is schematically depicted in Figure 2. Three bonds of the saturated cyclohexane ring are cleaved in a [2+2+2] ring opening procedure, giving rise to the 5-open or 6-open structures, depending on which set of three single bonds are broken. The model M system in the ONIOM treatment changes from cyclohexane to three separated $H_2C{=}CH_2$ entities, which are again closed shell systems and can be treated reliably at the chosen levels of theory. For the interaction and insertion of the metal cation, Li^+ is included in the M system.

A. Hexahydrofullerene, $C_{60}H_6$. This is the smallest system under investigation, and can be considered as a prototypical model, although it has never been synthesized.[27] Only AM1, PM3, and RHF/3-21G energetics were available for comparison.[9b] The closed **H6**, the 5-open **H6**−**5o** and the 6-open structure **H6**−**6o** all possess C_{3v} symmetry, as can be seen in Figure 1. The gain in energy due to hydrogenation to form **H6** from C_{60} and six isolated hydrogen atoms is calculated at the ONIOM-(G2MS) level to be 380.9 kcal/mol, i.e., 63.5 kcal/mol per C−H bond. As can be seen from Table 1, all open structures are higher in energy, with the 5-open structure **H6**−**5o** being more favorable by 7.1 kcal/mol relative to the 6-open structure **H6**−**6o**, which is 45.6 kcal/mol higher than **H6**. AM1 and PM3 place **H6**−**5o** at 9 to 14 kcal/mol higher than **H6**, and the relative energy for **H6**−**6o** is estimated to lie between 56 and 64 kcal/mol.[9] RHF/3-21G predicts more unfavorable energetics with **H6**−**5o** being 29.2 kcal/mol, and **H6**−**6o** about 76.8 kcal/mol higher in energy than **H6**, which means that the stability of the saturated ring system in **H6** is considerably overestimated as compared to ONIOM(G2MS) and the semiempirical methods. These numbers are somewhat lowered in BP/SVP calculations, which predict the relative energetics to be 19.5 kcal/mol (**H6**−**5o**) and 61.2 kcal/mol (**H6**−**6o**), respectively, and they are thus more in line with the most reliable ONIOM(G2MS) results. The larger stability of the 5-open structure over the 6-open structure is due to the fact that the former retains partially aromatic C_6 entities upon opening, as seen Figure 2, whereas the 6-open structure loses this additional stabilization, as suggested by the structures in Figure 2.

Table 3 lists the individual ONIOM(G2MS) energy components and S (substituent effect)[24] values for all open structures relative to **H6** and **M6**. Particularly interesting is the S(I−M)-value between system M and I for the 5-open structures, which is a measure of how much the surrounding environment of M influences its electronic structure. Although there is a rather small stabilizing effect from system R to system I (−6 and −9 kcal/mol for **H6** and **M6**, respectively), the stabilization increases to −28 kcal/mol when the electrons of system I are allowed to interact with the nearby electrons in system M. In contrast, there appears to be almost no corresponding stabilization for the 6-open structure, as shown in the very small S-values either for S(R−I) or S(I−M).

The carbon−carbon bonds in the hydrogenated six-membered ring are stretched from 1.459 Å in unmodified C_{60} to 1.596 Å in **H6** for bonds that are part of a five-membered ring, and from

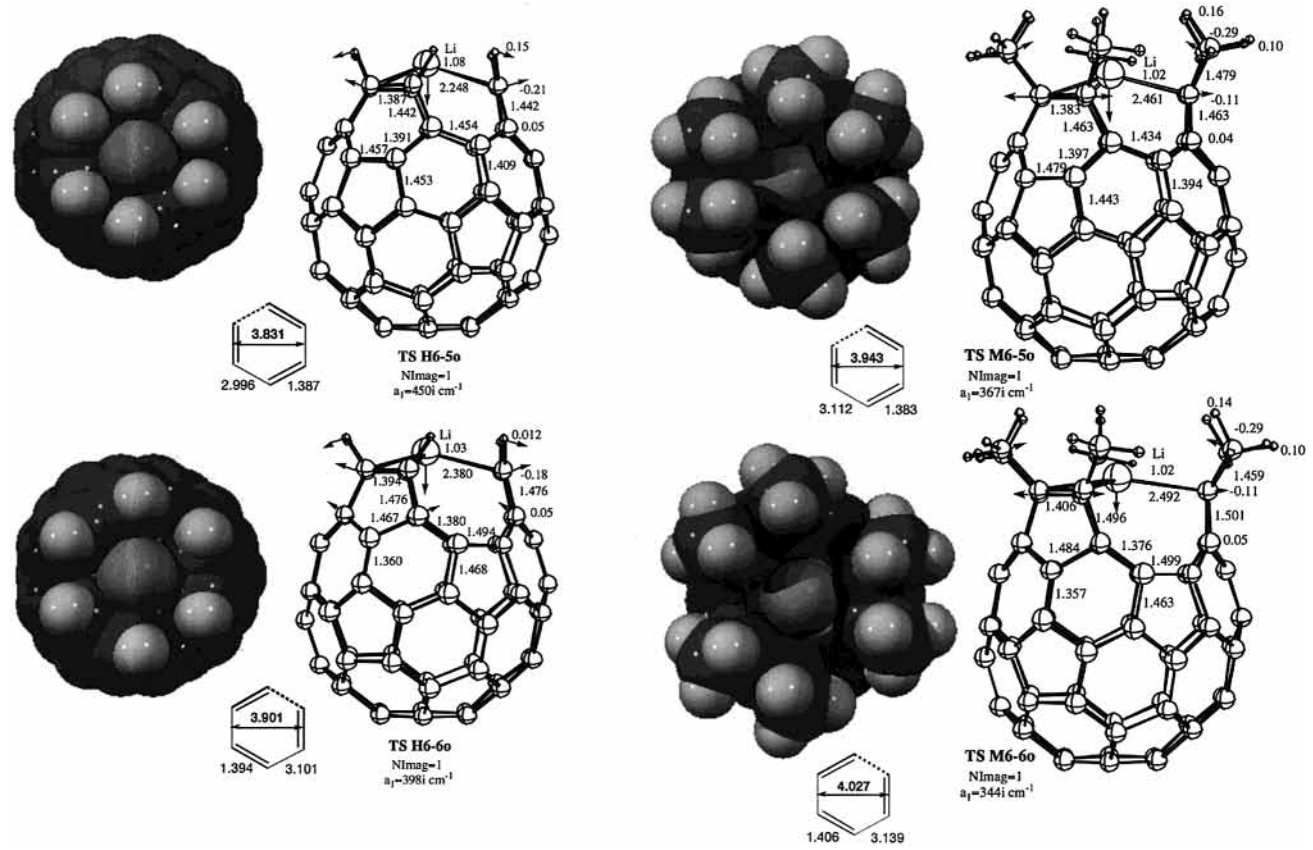

Figure 3. Transition states and reaction coordinate of Li^+ insertion for **H6**−**5o**, **H6**−**6o**, **M6**−**5o**, and **M6**−**6o**. Bond lengths are given in Å. Mulliken atomic charges from ONIOM2(MP2/6-31G(d):RHF/3-21G) calculations are given next to select atoms.

TABLE 3: Individual ONIOM Energy Contributions and Substituent Effects (in kcal/mol) for 5-Open (-5o) and 6-Open (-6o) Structures Relative to H6 and M6

ONIOM	**H6**	**H6**−**5o**	**H6**−**6o**	Δ (**6o**−**5o**)
E(R,L)	0	19.8	35.7	15.9
E(I,L)	0	25.7	36.3	10.6
E(I,M)	0	21.7	51.1	29.4
E(M,M)	0	50.1	53.3	3.2
E(M,H)	0	41.4	48.4	7.0
E(ONIOM3)	0	7.1	45.6	38.5
S(R−I)		−5.9	−0.6	5.3
S(I−M)		−28.4	−2.2	26.2
ONIOM	**M6**	**M6**−**5o**	**M6**−**6o**	Δ (**6o**−**5o**)
E(R,L)	0	14.6	30.0	15.4
E(I,L)	0	23.5	31.8	8.3
E(I,M)	0	19.5	45.1	25.6
E(M,M)	0	35.0	50.1	15.1
E(M,H)	0	25.7	44.0	18.3
E(ONIOM3)	0	1.3	37.2	35.9
S(R−I)		−8.9	−1.8	7.1
S(I−M)		−15.5	−5.0	10.5

1.408 to 1.591 Å for bonds that are part of a six-membered ring, respectively. This means that the six carbon−carbon bonds in **H6** are substantially longer than a typical carbon−carbon single bond. However, this ring stretch is by far not sufficient to provide an opening for an incoming metal atom or ion. The diameter of this six-membered ring, measured across the ring center between the center of two opposite carbon−carbon bonds of the six-membered ring, is only 2.87 Å, as shown in Figure 1. Assuming the covalent radius of 0.77 Å for carbon and the ionic radius of 0.76 Å for Li^+, the space available for a lithium cation to pass through the ring is estimated to be too small by 0.19 Å. In addition, one must realize that covalent radii give a very approximate measure for available space and that the interaction region of the carbon atoms with any approaching atom is much larger. Once the saturated six-membered ring is opened, the orifice becomes well developed. For instance, in 5-open structure **H6**−**5o** the alternating carbon−carbon distances on the opened ring are 1.385 and 2.911 Å (broken bond), which means that the three developed C═C bond lengths that reside in the six-membered rings are almost aromatic and the cleavages of the other three bonds is complete. The diameter of the distorted ring, measured as the distance between parallel bonded and nonbonded distances on either side of the opened six-membered ring, is now 3.72 Å and thus significantly wider than in **H6**. Going to the 6-open structure **H6**−**6o** increases this diameter even further to 3.85 Å, with alternating bond lengths of 1.378 and 3.012 Å, indicating a more localized double bond within the five-membered rings and a higher flexibility of the five-membered rings resulting in a pronounced bucket shape of the fullerene, as seen in Figure 1.

The structures of the transition states (TS's) for insertion of Li^+ into the 5-open and 6-open orifices are shown in Figure 3. These transition states are located where Li^+ comes closest to the six carbon atoms of the opened rings, with Li^+ being slightly above the center of the rings. The TS's are also of C_{3v} symmetry and have one a_1 imaginary frequency of 450*i* cm^{-1} (**H6**−**5o**) and 398*i* cm^{-1} (**H6**−**6o**). The reaction coordinate, shown in Figure 3, not only represents the insertion motion of Li^+ but also the motion for widening the orifice with CC stretches and bends. At both TS's the deformed six-membered rings actually have become even more open due to slight deformations in the opening region in order to accommodate the incoming ion. The insertion of Li^+ is required to overcome a very high barrier, which is, as shown in Table 1, 61.1 kcal/mol for **H6**−**5o** + Li^+ and 50.7 kcal/mol for **H6**−**6o** + Li^+. There exists a weak

initial complex with Li^+ being located 3.53 Å (**H6**−**5o**) and 3.78 Å (**H6**−**6o**) above the plane of the opened ring atoms, whereas the structure of the hydrocarbon skeleton is virtually unchanged. After the insertion barrier is overcome, another minimum with Li^+ inside the cavity was found in both cases, showing a stabilization energy of −10.8 kcal/mol (**H6**−**5o**) and −11.4 (**H6**−**6o**) below the dissociation limit. These minima are characterized by Li^+ being positioned almost exactly below the ring center, again giving rise to C_{3v} symmetry, with a distance of about 3.5 Å from the atoms of the ring opening. These ion-C_{60} interaction energies are surprisingly similar to those obtained by Geerlings et al.[12e] at the HF/3-21G level of theory with 9.4 kcal/mol after counterpoise correction [Their noncounterpoise corrected interaction energy is 27.7 kcal/mol. Due to the much larger basis sets we used for this ONIOM(G2MS) study, we expect the basis set superposition effect to be orders of magnitude smaller than for HF/3-21G.] for the $Li^+@C_{60}$ with the ion being located in the center of the cavity. Although it is known that ions can favor off-center positions in the endohedral complexes,[28] we did not attempt to locate such minima because the focus of this paper is more on the insertion step rather than to obtain accurate stabilization energies, which would also be somewhat arbitrary with the ONIOM model employed here.

We note that the barriers for entrance of even Li^+ as the smallest possible metal cation in these systems are too high, as expected from the steric encumbrance of Li^+. Larger openings are necessary in order to allow a metal atom or cation to enter the cavity of C_{60}, as will be discussed in the following sections.

B. Hexamethylfullerene, $C_{60}(CH_3)_6$. Increasing the size of the addend in the hexasubstituted C_{60} derivative is expected to enlarge the size of the orifice. Therefore, it is interesting to see the effect of replacing hydrogen by the bulkier methyl group, where steric interactions push all atoms of the opened rings even further apart. This system is also of hypothetical nature because it has not been synthesized, and serves only as a high-symmetry model for more easily accessible derivatives.

All structures for this system adopt C_{3v} symmetry as can be seen in Figure 1. The binding energy for the six methyl radicals is calculated to be 252.3 kcal/mol at the ONIOM(G2MS) level, i.e., 42.0 kcal/mol per methyl-carbon bond. This is substantially lower than that for the hydrogen−carbon bond in hydrogen substituted systems, which is indicative of the steric repulsion present in this system, as C−H and C−C bond energies are usually similar. Again, all open structures are higher in energy than **M6**, although the 5-open structure **M6**−**5o** is almost isoenergetic to **M6** at 1.3 kcal/mol at the ONIOM (G2MS) level (see Table 1). The 6-open structure **H6**−**6o** is higher in energy by 37.2 kcal/mol relative to **M6**, a difference similar to the 45.6 kcal/mol relative stability for the 6-open hydrogen system **H6**−**6o**. The semiempirical energies deviate more from the accurate ONIOM energies for the hexamethylfullerenes than for the hexahydrofullerenes. Both AM1 and PM3 predict that **M6**−**5o** should be more stable than **M6** by 36.4 and 19.4 kcal/mol, respectively, while ONIOM (G2MS) predicts this to be nearly thermoneutral. In the case of **M6**−**6o**, the semiempirical methods are again underestimating steric repulsion as compared to ONIOM (G2MS) by up to 37.2 kcal/mol. Thus, semiempirical methods seem to perform poorly in the case of strongly strained systems. BP/SVP calculations, on the other hand, predict these relative energies to be −3.7 kcal/mol (**M6**−**5o**) and 25.7 kcal/mol (**M6**−**6o**), respectively, which is more in line with our ONIOM results.

The steric repulsion within **M6** destabilizes this structure so much that the energy required for bond cleavage is gained by the relaxation that occurs during ring opening. However, inspection of Table 3 shows again that the S(I−M)-value (substituent value) between system M and system I for the 5-open structures is still largest with −15.5 kcal/mol, whereas some contribution comes also from S(R−I), since the deformations extend beyond the region of the intermediate model. The 6-open structure shows again rather small S-values with −1.8 kcal/mol (R−I) and −5.0 kcal/mol (I−M). This demonstrates once more that one major factor to describe the electronic structure of the open compounds is the aromaticity gained by ring opening in the 5-open structures, and that the 6-open structures are energetically not competitive.

Compared to **H6**, **M6** has even larger C−C bond lengths in the substituted ring with 1.657 and 1.668 Å, respectively. This is another indication that the entire system is under a high amount of strain, resulting in very elongated carbon−carbon single bonds, making this system highly unstable. However, the bond lengths in simple 1,2-substituted fullerenes are known to be unusually elongated, a fact usually attributed to the inherent strain of the fullerene framework.[29]

The closed structure **M6** is a true minimum on the potential energy surface, with no imaginary frequencies. Yet, the ring stretch is again not sufficient by itself to provide an opening for an incoming metal atom or ion. The diameter of this six-membered ring is 3.32 Å, which is comparable to the one of **H6**−**6o** with 3.72 Å. Openings of **M6**−**5o** and **M6**−**6o** are very similar with 3.86 and 3.97 Å, respectively, with somewhat longer C═C units of about 1.41 Å in the opening as compared to the hydrogenated species as a consequence of the steric repulsion of the methyl substituents.

Due to their larger openings, inserting Li^+ into the 5-open and 6-open orifices of the hexamethyl species **M6**−**5o** or **M6**−**6o** should require less energy than for **H6**−**5o** and **H6**−**6o.** This is particularly true for the 5-open system, where the energy of the Li^+ insertion transition state is reduced from 61.1 kcal/mol to 49.7 kcal/mol relative to the dissociation limit (see Figure 4). Going from **H6**−**6o** to **M6**−**6o** results in a less significant stabilization of the transition state, namely from 50.7 kcal/mol to 45.1 kcal/mol. The structures and vibrational eigenvectors for transition states are shown in Figure 3. The relatively similar energies for 5-open and 6-open hexamethyl substituted transition states are a reflection of the fact that the diameters of the six-membered opened rings are almost identical in the two transition states. Compared with those of the hexahydro species, these transition states are somewhat later in the reaction where Li^+ is almost coplanar with the six carbon atoms of the opened rings. They are also of C_{3v} symmetry and are associated with one a_1 imaginary frequency of $367i$ cm^{-1} (**M6**−**5o**) and $344i$ cm^{-1} (**M6**−**6o**).

As for initial complexes, we could not locate a minimum in the case of **M6**−**5o**. However, such a minimum exists for a weak initial complex with **M6**−**6o** and Li^+, which is located 4.57 Å above the plane of the opened ring atoms, whereas the structure of the hydrocarbon skeleton is virtually unchanged from **H6**−**6o**. Once the insertion barriers are overcome, another minimum with Li^+ situated inside the cavity was found in both cases, which shows a stabilization energy of −6.3 kcal/mol (**M6**−**5o**) and −7.1 (**M6**−**6o**) below the dissociation limit. The stabilization energies are of the same order as for **H6**−**5o** and **H6**−**6o**, indicating that the methyl substituents are no longer influencing the interaction of the metal atom with the C_{60} unit. Like in the hydrogenated systems, these minima are characterized by Li^+ being positioned almost exactly below the ring

center, again giving rise to C_{3v} symmetry, with a distance of about 3.5 Å from the atoms of the ring opening.

From these calculations, one can see that the barriers for entrance of Li^+ into these systems are still very high. Larger substituents or rigidifying addends as discussed in the Introduction seem to be necessary to increase the size of the orifice in order to allow a small metal atom or cation to enter the cavity of C_{60}. Effecting higher numbers of bond scissions is also an alternative that will need to be achieved through experimental protocols.

C. Bistriazoline and Bislactam Derivatives. The bistriazoline derivative **N3** and the bislactam derivative **NCO** (see Figure 1) are members of a series of compounds that have been proposed as more practical systems for organic synthesis, while being also much more widely open. Interestingly, in attempts to synthesize **N3**, the unexpected derivative **NCO** was obtained experimentally by Rubin et al.[9] This latter compound displays the largest ring opening of any synthesized fullerene (>4 Å). Both the hypothetical (**N3**) and the synthesized (**NCO**) compounds have in common that they are derived by addition of 1,4-bis(2-azidophenyl)butadiene $(N_3)\phi-C_4H_4-\phi(N_3)$, ϕ = *o*-C_6H_4, to C_{60}, which provides a rigid, computationally designed framework that serves as the backbone of the functionalized ring system. Due to the symmetric nature of the addends, both systems are C_s symmetric before interaction with metal ions. However, interaction of incoming metal ions with the functional groups attached to the ring opening may lead to breaking of the symmetry, as will be shown for the case of **NCO**. The hypothetical **N3** features the same type of orifice as the hexahydro- and hexamethylfullerenes, namely a 5-open structure featuring benzene and triazole moieties derived from three cycloaddition reactions with the six-membered ring double bonds, as shown in Figure 2. Therefore, the six-membered ring was chosen to be the same high level model system M as employed for the previous systems, with the six nitrogen atoms added to the intermediate system I and the remainder of the macrocycle was treated in the R system only (see Table 2). The experimentally obtained **NCO**, on the other hand, does not fall into a 5 or 6-open category, but could be best described as a system in which a single C═C bond was separated from the remaining four atoms of the six-membered ring, as shown in Figure 2. These four carbon atoms form a bisamide moiety and are represented by a malealdehyde unit OHC−CH═CH−CHO in the high level model system M, together with an ethylene unit for the remaining two carbon atoms of the opened ring. The reason for inclusion of oxygen into M is that double bonds of the real system should not be replaced by single bonds in any model, and to keep the terminal carbon atoms sp^2 hybridized. Because this can be achieved already with keeping oxygen in the model system, cutting at the partially conjugated C−N bonds is certainly not a dramatic oversimplification. These bridging nitrogen atoms were included in the intermediate system I, and the remainder of the macrocyle was treated in the R system only, as in **N3**.

As the functional groups added to C_{60} are chosen to be larger, it becomes more difficult to specify a single number as a measure of the size of the ring opening due to additional steric requirements of these groups which may hinder the entrance of a metal atom or ion. The diameter defined above for the six-membered opened ring (distance between parallel bonded and nonbonded C−C distances) can be used for **N3** and is calculated at the ONIOM2 level to be 4.02 Å. The opening of **NCO** can be calculated as the distance between parallel C−C double bonds on either side of the six-membered ring, and is about 4.11 Å.

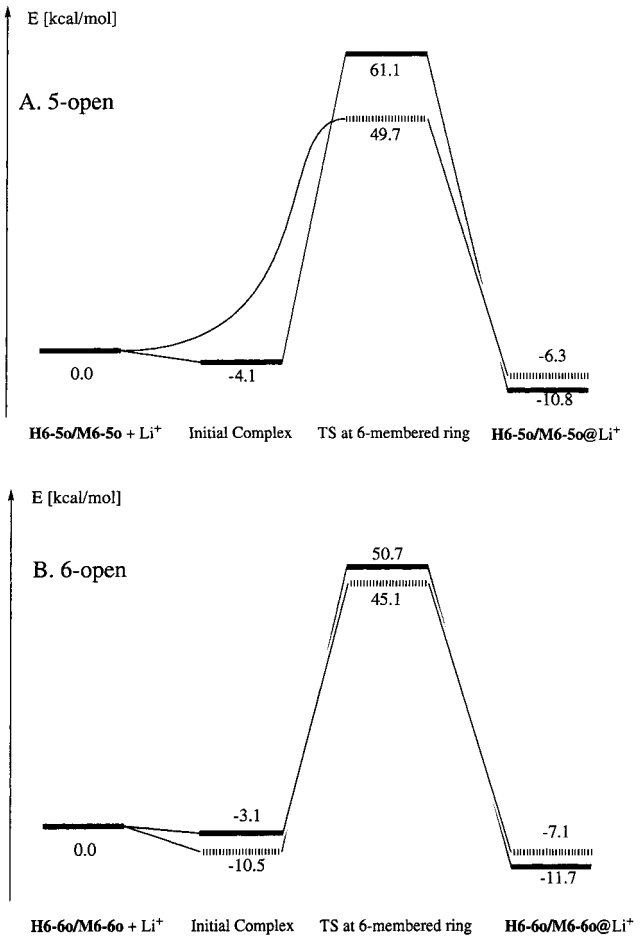

Figure 4. Energy profiles of Li^+ insertion for (A). **H6**−**5o** and **M6**−**5o**, and (B). **H6**−**6o** and **M6**−**6o**. ONIOM(G2MS) relative energies are given with respect to **H6** + Li^+ and **M6** + Li^+ and are in kcal/mol.

The rigidity of the macrocycle and the larger openings make them more realistic candidates for metal atom insertions. The structures of the Li^+ insertion transition states are in fact, as shown in Figure 5, not much different from those of the systems without metal ions, in clear contrast to the **H6** and **M6** systems previously discussed. These structural characteristics are reflected in the lower barriers toward Li^+ entrance. The energy of the transition state for **N3** is just 19.6 kcal/mol above the dissociation limit at the ONIOM(G2MS) level, and the imaginary frequency obtained for this structure is 375*i* cm^{-1}. BP/SVP predicts a relative energy of 24 kcal/mol, which is in reasonable agreement with ONIOM(G2MS). The real transition state for **NCO** was found in C_1 symmetry, as the stationary point in C_s symmetry is a secondary saddle point, one of the imaginary frequencies being of *a″* symmetry at 127*i* cm^{-1}. Following its displacement vector, we found the true transition state shown in Figure 5. It is characterized by strong interaction between Li^+ and one of the negatively charged oxygen atoms of the amide groups, where Li^+−O distances are 2.788 and 3.107 Å, respectively. This transition state for **NCO** is even lower in energy than the one for **N3**, lying only 15.7 kcal/mol higher (BP/SVP: 23 kcal/mol) in energy than the reactants, with an associated imaginary frequency of 344*i* cm^{-1}. The reaction coordinates for both transition states consist of the CC stretches and bends for widening the orifice as well as the Li^+ insertion motion, as in transition states for the other systems above.

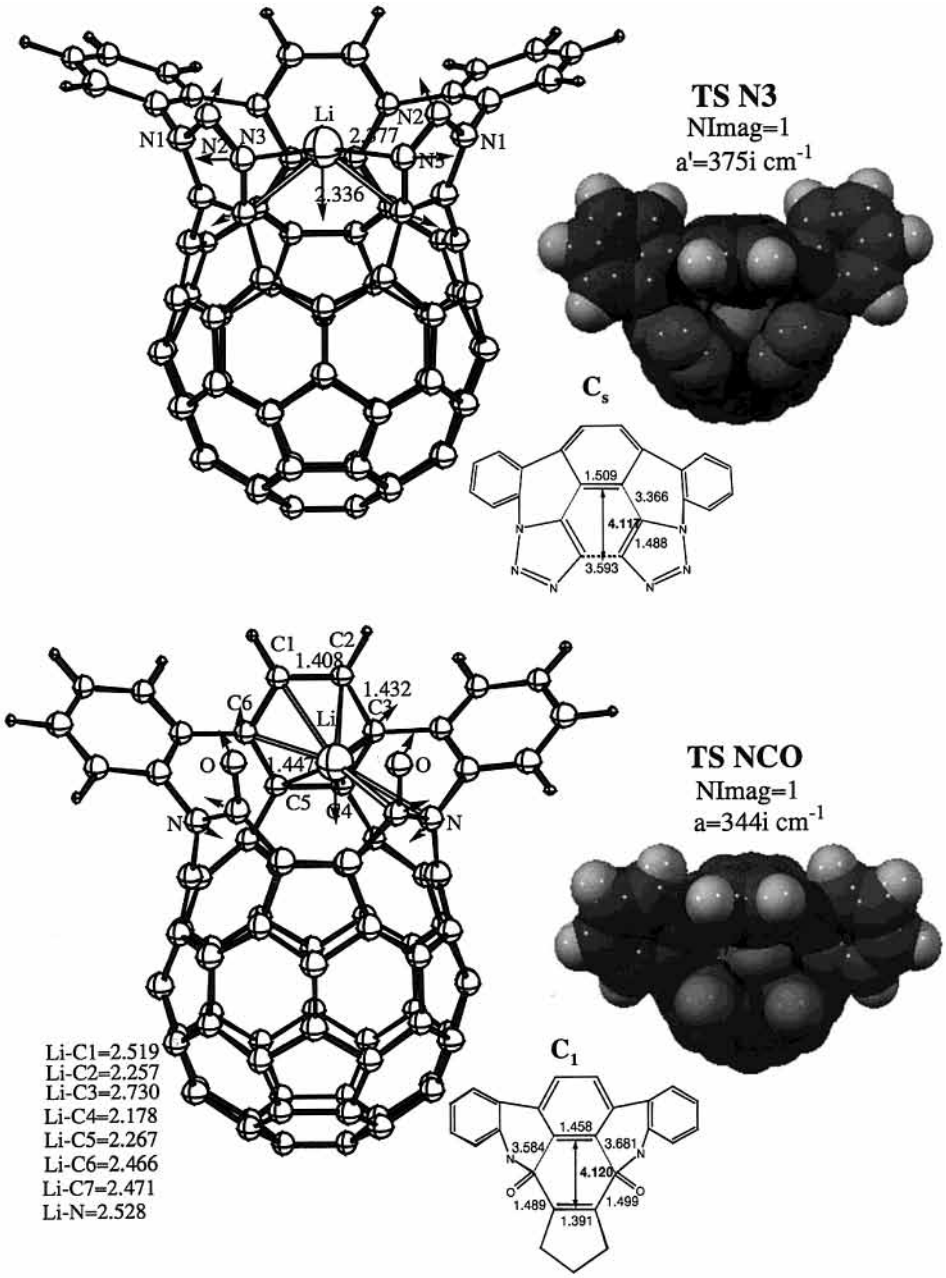

Figure 5. Transition states and reaction coordinate of Li^+ insertion for **NCO** and **N3**. Bond distances are given in Å.

IV. Conclusions

Using the ONIOM method, we have studied the relative stabilities of 5- and 6-open derivatives of C_{60} and transition states for Li^+ insertion at a level comparable to the very accurate G2MS, where hydrogen, methyl, and macrocycles were chosen as functional groups that are involved in retro [2+2+2] cycloaddition reactions, as proposed by Rubin et al.[3,9] Two-layer ONIOM(MP2/6-31G(d):RHF/3-21G) was used for geometry optimizations and frequency calculations, and single point energy calculations have been performed using three-layer ONIOM(G2MS:MP2/6-31G(d):RHF/3-21G), where usually the opened six-membered ring atoms were treated at the G2MS level of theory.

The ONIOM (G2MS) finds that the 5-open hexahydro species **H6**−**5o** is much more stable than the 6-open species **H6**−**6o** and is only several kcal/mol endothermic relative to **H6**. The extra stability of the 5-open species over the 6-open analogue can be attributed to the aromatic stability of the six-membered rings retained in the orifice by the opening of the 5-memebred ring (see Figure 2). Semiempirical (AM1 and PM3) results agree quite well with the ONIOM results for these species. The ONIOM (G2MS) finds the 5-open hexamethyl species **M6**−**5o** slightly higher in energy than the closed form **M6**. This is in strong contrast to the semiempirical results, which indicate that the 5-open species is 20−36 kcal/mol more stable than the closed form; the semiempirical methods seem to be vastly overestimating the steric strain of the closed form.

Barriers for entrance of Li^+ as the smallest possible metal cation into these open structures were calculated to be extremely high with relative energies of 61.1 kcal/mol (**H6**−**5o**) and 50.7 kcal/mol (**H6**−**6o**), respectively. These barriers are somewhat reduced when hydrogen is replaced by methyl, making the orifices larger due to steric repulsion and the insertion step easier with relative energies of 49.7 kcal/mol for **M6**−**5o** and 45.1 kcal/mol for **M6**−**6o**, respectively. In either case, the orifice is not large enough for the smallest ion to go through.

The macrocyclic bistriazoline and bislactam systems, **N3** and **NCO**, studied as examples for systems that can be prepared experimentally, gives slightly larger orifices and substantially smaller barriers for Li^+ insertion, compared to the hypothetical systems described above, i.e., 20 and 16 kcal/mol for **N3** and **NCO**, respectively. This barrier is in the range accessible under relatively mild conditions. Given the fact that Li^+ is the smallest member of metal cations, and that transition metal atoms such as Co are roughly three times larger, it remains an open question as to how the orifice diameter could be even further increased.

Acknowledgment. The authors are grateful to Dr. Thom Vreven for discussions and assistance in using the ONIOM method and codes. The present research is in part supported by grants CHE-9627775 (K. M.) and CHE-0080942 (Y. R.) from the National Science Foundation. Acknowledgment is made to the Cherry L. Emerson Center of Emory University for the use of its resources, which is in part supported by a National Science Foundation Grant No. CHE-0079627 and an IBM Shared University Research Award. Acknowledgment is also made for generous support of computing time at the National Center for Supercomputing Applications (NCSA).

References and Notes

(1) Dresselhaus, M. S.; Dresselhaus, G.; Eklund P. C. In *Science of Fullerenes and Carbon Nanotubes*; Academic Press: San Diego, 1995.

(2) (a) Hebard, A. F.; Rosseinsky, M. J.; Haddon, R. C.; Murphy, D. W.; Glarum, S. H.; Palstra, T. T. M.; Ramirez, A. P.; Kortan, A. R. *Nature* **1991**, *350*, 600. (b) Holczer, K.; Klein, O.; Huang, S. M.; Kaner, R. B.; Fu, K. J.; Whetten, R. L.; Diederich F. *Science* **1991**, *252*, 1154.

(3) Rubin Y. *Chem. Eur. J.* **1997**, *3*, 1009.

(4) (a) Suzuki, T.; Maruyama, Y.; Kato, T.; Kikuchi, K.; Achiba, Y.; Kobayashi, K.; Nagase S. *Angew. Chem., Int. Ed. Engl.* **1995**, *35*, 2234. (b) Ding J.; Yang S. *Angew. Chem., Int. Ed. Engl.* **1996**, *35*, 2234. (c) Shinohara, H.; Inakuma, M.; Hayashi, N.; Sato, H.; Saito, Y.; Kato, T.; Bandow S. *J. Phys. Chem.* **1994**, *98*, 8597. (d) Shinohara, H. *Rep. Prog. Phys.* **2000**, *63*, 843. (e) Nagase S.; Kobayashi, K.; Akasaka, T. *Bull. Chem. Soc. Jpn.* **1996**, *69*, 9, 2131. (f) Akasaka, T. *J. Am. Chem. Soc.* **2000**, *122*, 9316. (g) Stevenson, S.; Rice, G.; Glass, T.; Harlch, K.; Cromer, F.; Jordan, M. R.; Craft, J.; Hadju, E.; Bible, R.; Olmstead, M. M.; Maltra, K.; Fisher, A. J.; Balch, A. L.; Dorn, H. C. *Nature* **1999**, *401*, 55.

(5) Rohmund, F.; Bulgakov, A. V.; Heden, M.; Lassesson, A.; Campbell, E. E. E. *Chem. Phys. Lett.* **2000**, *323*, 173.

(6) For a recent report on $Er@C_{60}$ isolated in aniline solution, see: Ogawa, T.; Sugai, T.; Shinohara, H. *J. Am. Chem. Soc.* **2000**, *122*, 3538.

(7) Aree, T.; Hannongbua, S. *Chem. Phys. Lett.* **1997**, *260*, 427.

(8) (a) Braschwitz, W.-D.; Otten, T.; Rücker, C.; Fritz, H.; Prinzbach, H. *Angew. Chem., Int. Ed. Engl.* **1989**, *28*, 1348. (b) Mohler, D. L.; Vollhardt, K. P. C.; Wolff, S. *Angew. Chem., Int. Ed. Engl.* **1990**, *29*, 1151.

(9) (a) Schick, G.; Jarrosson, T.; Rubin, Y. *Angew. Chem., Int. Ed. Engl.* **1999**, *38*, 2360. (b) Rubin, Y. *Top. Curr. Chem.* **1999**, *199*, 67.

(10) Rubin, Y.; Ganapathi, P. S.; Franz, A.; An, Y.-Z.; Qian, W.; Neier, R. *Chem. Eur. J.* **1999**, *5*, 3162.

(11) Rubin, Y.; Jarrosson, T.; Wang, G.-W.; Bartberger, M. D.; Schick, G.; Saunders, M.; Cross, R. J.; Houk, K. N. *Angew. Chem., Int. Ed. Engl.* **2001**, *40*, 1543.

(12) (a) Andreoni, W. *Annu. Rev. Phys. Chem.* **1998**, *49*, 405. (b) Bauernschmitt, R.; Ahlrichs, R.; Hennrich, F. H.; Kappes, M. M. *J. Am. Chem. Soc.* **1998**, *120*, 5052. (c) Stener, M.; Fronzoni, G.; Venuti, M.; Decleva, P. *Chem. Phys. Lett.* **1999**, *309*, 129. (d) Aree, T.; Kerdcharoen, T.; Hannongbua, S. *Chem. Phys. Lett.* **1998**, *285*, 221. (e) De Proft, F.; Van Alsenoy, C.; Geerlings, P. *J. Phys. Chem.* **1996**, *100*, 7440.

(13) (a) Boese, A. D.; Scuseria, G. E. *Chem. Phys. Lett.* **1998**, *294*, 233. (b) v. Wüllen, C. *Chem. Phys. Lett.* **1994**, *219*, 8. (c) Patchkovskii, S.; Thiel, W. *J. Chem. Phys.* **1997**, *106*, 1796.

(14) Curtiss, L. A.; Raghavachari, K.; Trucks, G. W.; Pople, J. A. *J. Chem. Phys.* **1991**, *94*, 7221.

(15) Curtiss, L. A.; Raghavachari, K.; Pople, J. A. *J. Chem. Phys.* **1993**, *98*, 1293.

(16) Dapprich, S.; Komaromi, I.; Byun, K. S.; Morokuma, K.; Frisch, M. J. *J. Mol. Struct. (THEOCHEM)* **1999**, *461*−*462*, 1.

(17) Froese, R. D. J.; Humbel, S.; Svensson, M.; Morokuma, K. *J. Phys. Chem.* **1997**, *101A*, 227.

(18) Shannon, R. D. *Acta Crystall., Section A* **1976**, *32*, 751.

(19) (a) Becke, A. D. *Phys. Rev. A* **1988**, *38*, 3098. (b) Perdew, J. P.; Zunger, A. *Phys. Rev. B* **1981**, *23*, 5048.

(20) Schäfer, A.; Horn, H.; Ahlrichs, R. *J. Chem. Phys.* **1992**, *97*, 2571.

(21) Häser, M.; Ahlrichs, R. *J. Comput. Chem.* **1989**, *10*, 104.

(22) Eichkorn, K.; Treutler, O.; Öhm, H.; Häser, M.; Ahlrichs, R. *Chem. Phys. Lett.* **1995**, *242*, 652.

(23) Froese, R. D. J.; Morokuma, K. *Chem. Phys. Lett.* **1999**, *305*, 419.

(24) Vreven, T.; Morokuma, K. *J. Comput. Chem.* **2000**, *21*, 1419.

(25) Vreven, T.; Morokuma,K. *J. Chem. Phys.* **1999**, *111*, 8799.

(26) Frisch, M. J.; Trucks, G. W.; Schlegel, H. B.; Scuseria, G. E.; Robb, M. A.; Cheeseman, J. R.; Zakrzewski, V. G.; Montgomery, J. A.; Stratmann, R. E.; Burant, J. C.; Dapprich, S.; Millam, J. M.; Daniels, A. D.; Kudin, K. N.; Strain, M. C.; Farkas, O.; Tomasi, J.; Barone, V.; Cossi, M.; Cammi, R.; Mennucci, B.; Pomelli, C.; Adamo, C.; Clifford, S.; Ochterski, J.; Petersson, G. A.; Ayala, P. Y.; Cui, Q.; Morokuma, K.; Malick, D. K.; Rabuck, A. D.; Raghavachari, K.; Foresman, J. B.; Cioslowski, J.; Ortiz, J. V.; Stefanov, B. B.; Liu, G.; Liashenko, A.; Piskorz, P.; Komaromi, I.; Gomperts, R.; Martin, R. L.; Fox, D. J.; Keith, T.; Al-Laham, M. A.; Peng, C. Y.; Nanayakkara, A.; Gonzalez, C.; Challacombe, M.; Gill, P. M. W.; Johnson, B.; Chen, W.; Wong, M. W.; Andres, J. L.; Head-Gordon, M.; Replogle, E. S.; Pople, J. A. *Gaussian 98*; Gaussian, Inc.: Pittsburgh, PA, 1998.

(27) For related tetrahydro- and hexahydrofullerenes, see: Bergosh, R. G.; Meier, M. S.; Cooke, H. P.; Spielmann, J. A. L.; Weedon, B. R. *J. Org. Chem.* **1997**, *62*, 7667, and references therein.

(28) (a) Cioslowski, J.; Fleischmann, E. *J. Chem. Phys.* **1991**, *94*, 3739. (b) Breton, J.; Gonzalez-Platas, J.; Girardet, C. *J. Chem. Phys.* **1993**, *99*, 4036.

(29) Hirsch, A. *The Chemistry of the Fullerenes*; Thieme Verlag: Stuttgart, 1994.